AD-A066 694   NAVY ELECTRONICS LAB SAN DIEGO CALIF   F/G 20/1

LONG-RANGE SHALLOW-WATER PROPAGATION LOSS FLUCTUATIONS, (U)

1958   K V MACKENIZE

UNCLASSIFIED   NL

1 OF 1

AD A066894

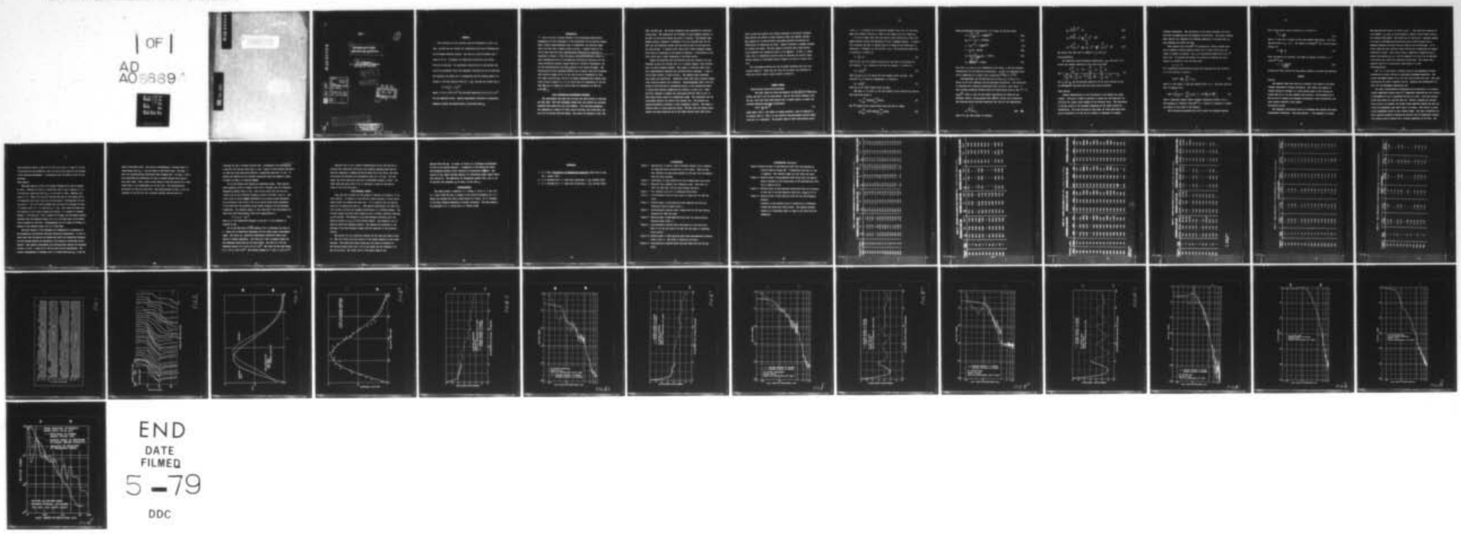

END

DATE FILMED

5-79

DDC

LEVEL II

(1)

(6) LONG-RANGE SHALLOW-WATER PROPAGATION LOSS FLUCTUATIONS,

(10) K. V. Mackenzie
U. S. Navy Electronics Laboratory
San Diego 52, California

(12) 45 p.

(11) 1958

The opinions and assertions contained herein are the private ones of the writer, and are not to be construed as official, or as reflecting the views of the Navy Department or the naval service at large.

253 550

ABSTRACT

The fluctuation of the received sound for frequencies of 350, 700, 1200, and 2400 cps was studied for transmission over flat 60-fathom sand and 50-fathom sandstone bottoms. The received sound fluctuated over a range of 50 db. In general, the amplitude distribution was neither Gaussian or Rayleigh. No significant correlation was found between the receiving hydrophones which were separated vertically by 100 or more feet. The frequency was spread due to transmission and the relative power P is related to the half spectra width, $\left| f - f_o \right|$ from 350 cps to 2400 cps by

$$P = bf_o \left| f - f_o \right|^{-3}$$

where $b = (7.7 \pm 0.8) \times 10^{-6}$ for the sand bottom and $(13.9 \pm 2.7) \times 10^{-6}$ for the sandstone bottom. Special measurements indicated no significant asymmetry between the spectra above f_o from that below f_o.

INTRODUCTION

One of the most striking features of the long-range shallow-water propagation of sonic frequencies is the fluctuation of the received signals. When a steady single-frequency tone is transmitted, the received signal level will vary over a range as much as 50-db. A typical record of received sound which has been logarithmically amplified and rectified is reproduced in Figure 1. The fluctuation characteristics of a typical record of received sound were studied to yield information about (1) the amplitude distribution functions, (2) the cross-correlations between signals received at different hydrophones, and (3) the autocorrelations and power spectra of the signal envelopes. The shallow-water results presented here are for an almost ideal flat 60-fathom sand bottom at ranges of 10, 15, 20, and 30 kyd for frequencies of 350, 700, 1200, and 2,400 c/s; and for a 50-fathom nondepositional miocene sandstone bottom at ranges of 4, 8, 16, and 25 kyds for frequencies of 700 and 1200 c/s; and, at ranges of 4 and 16 kyds for frequencies of 1200 and 2,400 c/s. cps

FIELD TRANSMISSION MEASUREMENTS PROCEDURE

The measurements were made over two flat and level bottoms in February and June 1958. Only four hydrophone depths were used because the available automatic data reader had only four channels. One receiving hydrophone was suspended at a depth of 10 feet, one at 100 feet, one at 200 feet, and one at 10 to 20 feet from the bottom. The source was operated at 350, 700,

1200, and 2400 cps. The source frequencies were controlled by protected tuning forks. The frequencies are estimated to have remained constant to one part in one million during any given 5.5 minutes. The maximum range change during 5.5 minutes is estimated to be less than 200 feet for the data over the sandstone bottoms and less than 50 feet for the data over the sand bottoms. A constant drift would cause a small frequency change which would be undetected by the method of analysis. A fluctuation of the drift could cause a small broadening of the power spectra.

Aboard the receiving ship the received sound was filtered by 30 cps band-pass filters and recorded both on a 7-channel magnetic tape recorder, and on an Edin 6-channel recorder. The signals on the Edin inked record were logarithmically amplified and rectified before recording. A copy of one of these records is shown on Fig.1. The magnetic-tape recordings were linear and unrectified. Immediately after each long 5.5-minute signal, every receiving channel was calibrated. Bathythermographs (BT's) were obtained at both ends and at intermediate points of the transmission paths to obtain more accurate temperature and salinity vs depth data. These data were combined to compute the sound-speed profiles shown in Fig. 2. This figure should really be 3-dimensional graph. The coordinates for the sound-speed profiles are shown at the extreme left. The profiles are spaced horizontally according to their geographic location. The range in nautical miles is shown along the bottom. The BT's were not always evenly spaced; the marks along the top of the graph indicate where 4900 ft/sec

lined up when the profiles were spaced according to the actual distances. Some profiles are dashed to avoid confusion where the profiles overlap. This typical set of shallow-water sound-speed profiles illustrates the difficulties of idealizing the ocean. Figure 2 exhibits a somewhat systematic change with range. The best method of deciding what single profile could represent the transmission path is not apparent. In fact, it seems likely that a 4-dimensional picture would be necessary for precise computations because of sound-speed profile changes with time at a given location.

The sound-speed profiles for the 50-fathom sandstone area were only slightly negative. Rough seas and time did not permit the obtaining of sufficient data to make a figure similar to Figure 2.

GENERAL THEORY

Sound Pressure Distribution Functions

The water depth for these measurements was for the 300 ft sandstone bottom, and 360 ft for the sand bottom. Even at the lowest frequency used, 350 cps, there were many modes present and it seemed logical to expect the classical Rayleigh expression (normalized)

$$F(x) = \frac{2x}{a} \exp^{-\frac{x^2}{a}} \tag{1}$$

might apply since n, the number of random variables, could be expected to be greater than 10. Here x is the received root-mean-square pressure amplitude and a is a parameter. The general shape of these distribution curves

in Fig. 3. A truncated ($x \geq o$) Gaussian (normal) curve with the same area, mean, and standard deviation is shown by the dashed curve for comparison.

It will be shown later that the results yield distribution curves that appear Gaussian rather then Rayleigh, but are in general neither. A logical way to present the data in tabular form is in terms of the coefficient of variation, V; skewness, a_3; and kurtosis, a_4-3. The population coefficient of variation is defined as

$$V = \frac{\sigma}{m} 100 , \tag{2}$$

where σ and m are the standard deviation and the mean of the population. The skewness,[1] a_3, a measure of the lack of symmetry, is defined as

$$a_3 = m_3/m_2^{3/2} \tag{3}$$

where m_2 and m_3 are the second and third moments about the mean. The kurtosis,[1] a_4, a measure of peakedness, is defined as

$$a_4 = m_4/m_2^{2} , \tag{4}$$

where m_4 is the fourth moment about the mean.

The mean, m, of course is the first moment of the distribution function F(x) about the origin or

$$m = \int_{-\infty}^{\infty} xF(x)dx \Big/ \int_{\infty}^{\infty} F(x)dx. \tag{5}$$

The k^{th} moment of any function F(x) about the mean is simply

$$m_k = \int_{-\infty}^{\infty} (x-m)^k F(x)dx \Big/ \int_{-\infty}^{\infty} F(x)dx. \tag{6}$$

Using the Rayleigh distribution Eq. (1) in Eqs. (5) and (6) yields

$$m = \frac{\pi^{1/2} a^{1/2}}{2} = 0.88623a^{1/2}, \tag{7a}$$

$$m_2 = \left(1 - \frac{\pi}{4}\right) a = 0.21460a \ , \tag{7b}$$

$$\sigma = m_2^{\ 1/2} = 0.46325a^{1/2}, \tag{7c}$$

$$V = \frac{\sigma}{m} 100 = 52.27\% \tag{7d}$$

$$a_3 = \frac{2\pi^{1/2}(\pi - 3)}{(4-\pi)^{3/2}} = 0.63111 \ , \tag{7e}$$

$$a_4 = \frac{32-3\pi^2}{(4-\pi)^2} = 3.24509 \ . \tag{7f}$$

Note that V, a_3 and a_4, are independent of the value, a, and are constants characteristic of all Rayleigh distributions. In fact, all Rayleigh curves can be normalized to a single curve by plotting $a^{1/2}F(x)$ vs $a^{-1/2}x$.

Correspondingly for the Gaussian distribution, $a_3 = 0$ and $a_4 = 3$. These are not very different from the Rayleigh distribution. The coefficient of variation for a Gaussian distribution does not have a given value. A more striking difference between these two distributions would be ~~for~~ shown by $m_5/m_2^{5/2}$, which is zero for the normal distribution but large for the Rayleigh; however, the ~~xx~~ present data doe~~s~~ not justify this elaboration. The following easily derivable equations were used for the computations:

$$m = \frac{1}{N}\sum_{i=1}^{N} x_i \ , \tag{8a}$$

where N is the total number of readings.

$$m_2 = \frac{1}{N} \sum_{i=1}^{N} x_i^{\,2} - m^2 \tag{8b}$$

$$m_3 = \frac{1}{N} \sum_{i=1}^{N} x_i^{\,3} - \frac{3m}{N} \sum_{i-1}^{N} x_i^{\,2} + 2m^3 \tag{8c}$$

$$m_4 = \frac{1}{N} \sum_{i=1}^{N} x_i^{\,4} - \frac{4m}{N} \sum_{i=1}^{N} x_i^{\,3} + \frac{6m^2}{N} \sum_{i=1}^{N} x_i^{\,2} - 3m^4 \tag{8d}$$

The results were then used to compute V, a_3, and a_4-3.

Cross-Correlation

The normalized cross-correlation coefficients, r_{12}, were used to determine the spatial coherence of the sound field where

$$r_{12} = \frac{N \sum_{j=1}^{N} x_{1j} \; x_{2j} - \sum_{j=1}^{N} x_{1j} \sum_{j=1}^{N} x_{2j}}{\left\{ \left[N \sum_{j=1}^{N} x_{1j}^{2} - \left(\sum_{j=1}^{N} x_{1j} \right)^2 \right] \left[N \sum_{j=1}^{N} x_{2j}^{2} - \left(\sum_{j=1}^{N} x_{2j} \right)^2 \right] \right\}^{\frac{1}{2}}} \tag{9}$$

and x_{1j} and x_{2j} are the pressure amplitudes of the sound received on the two hydrophones from which data are being cross-correlated.

Power Spectra

Another characteristic of the fluctuation is how rapidly the signal changes. Obviously it might be possible to obtain the same amplitude distribution for signals which changed at far different rates. The fluctuation is chiefly caused by the frequency broadening of the signal during the transmission. The sound arriving at long range for these many-modes cases may be considered to be the sum of a number of components of slightly

different frequencies. The fluctuation of the signal envelopes can result from both the amplitude and the frequency distributions. The signal envelope power spectra will represent the frequency spreading if the amplitudes for each frequency are almost the same.

Power spectra were obtained[2,3] by choosing the interval between readings to examine a desired spectral width, and to obtain resolution, and number of degrees of freedom. Let x_j, be the pressure amplitude of the j^{th} value used. To minimize the effects of starting and stopping the data, change to a variable y about the mean where

$$y_j = x_j - m.$$

The unnormalized autocorrelation $R_{11}(p)$ which measures the time variability in one location is given by

$$R_{11}(p) = \frac{1}{N-p} \sum_{j=1}^{N-p} y_j y_{j+p} \tag{10}$$

where p is the number of lags (an integer) from 0 to q. The power spectrum U(h) is computed from

$$U(h) = \frac{1}{q}\left[R_{11}(0) + \sum_{p=1}^{q-1} R_{11}(p) \left(1 + \cos\frac{\pi p}{q}\right)\cos\frac{\pi hp}{q}\right] \tag{11}$$

where h represents equally spaced integral frequencies between 0 and q. The smoothing or "hanning" function[2,3] $(1 + \cos\pi p/q)$ is necessary to reduce the effect of side lobes in the analysis.

The following relationship was used to select the reading interval.

There are q equally spaced frequencies at intervals of

$$\Delta f = \frac{1}{2q\tau} \tag{12}$$

where τ is the time in seconds between the selected data points. The total spectrum width is $f_m = q \Delta f$. The degrees of freedom,[2,3] for initial program design, are

$$k = \frac{2N}{q} - \frac{2}{3} . \tag{13}$$

After the spectra are obtained, the number of degrees of freedom, k' is computed[2,3] from

$$k' = \frac{(\Sigma\, U(h))^2}{\Sigma\, U^2(h)} . \tag{14}$$

Blackman and Tukey utilize the Chi-squares behavior to discuss the precision.

RESULTS

Analysis

The magnetic tapes were read on an automatic data reader at the Naval Ordnance Laboratory at Corona, California. This reader was capable of reading varying dc voltages at a total maximum speed of 400 readings per second when all of its four channels were utilized. The Burroughs 205 at NEL was used to compute the frequency distribution, cross-correlations, and power spectra included in this report.

Distribution Curves

The frequency distribution curves or histograms were plotted and showed considerable variability. Some were Gaussian. A few appeared to be more

more Rayleigh distributed, as shown in Fig. 4. The statistical measures of curve shape V, a_3, and a_4-3 are presented in Tables I and II which utilize four million data points. The coefficient of variation V, sometimes appears to be near to the Rayleigh distribution value of 52.27 percent but is markedly different from this value for many of the distributions. It is always large and this indicates large fluctuations in amplitude for signals received at a point. The kurtosis factor, expressed as departure from a normal distribution by a_4-3, could be expected to be zero for the Gaussian distribution and +0.245 for a Rayleigh distribution. This factor has a negative value for a surprisingly large number of curves.

Cross-Correlation

Sea time did not permit a detailed study of the dependence of cross-correlation on either vertical or horizontal hydrophone separation. The regular hydrophone depths of 10, 100, 200, and 345 feet were used. The cross-correlations are given in Tables V and VI. Generally the correlations are small for the hydrophone separations used.

Any small crosscorrelation coefficient can be considered to be mathematically significant because about 10^4 independent determinations are involved. A correlation of 0.03 is significant at the 0.01 level. Note that actually 30,000 data points are used per data set. However, although the readings were at every 0.01 seconds, the 30-cps filter bandwidth smooths the data and yields an independent value about every 0.03 second. This results in about 10,000 independent values in the 5 minute sample. The small correlations do have a physical meaning by showing the definite lack of significant correlation between sound at points with a vertical separation of 100 feet. The

high correlation shown in Table VI for 2400 cps sound at a range of 16 kyds is attributed to the probability that the narrow sound beam was not centered on the receiving hydrophones. Corresponding data for Tables II and IV were discarded.

Power Spectra

The power spectrum width of the signal envelope could only be guessed at first. Readings at every 0.1 second were used to get a spacing of Δf = 0.05 cps and a spectrum width of f_m = 5 cps with N = 3000. Equation (13) gives k = 59. These first results indicate that most of the energy occurs at frequencies less than 1 cps, and the resulting k' from Equation (14) was only about 7. For this reason another pass was made with readings at every 0.5 second to get Δf - 0.01 cps and f_m = 1 cps. This value of T gave only 600 readings in the 5-minute sample and yielded k = 11 degrees of freedom; however, k' was about 20. For 11 degrees of freedom, the chi-square analysis indicates that the spectral values lie in a 6.3-db band about the estimated value 90 percent of the time. Correspondingly for 20 degrees of freedom, 90 percent of the observed values lie in a 4.6-db band.

The power spectra of the envelopes are interpreted as a broadening of the frequency by some process occurring during the transmission. It will be shown later that the spectra are symmetrical about the transmitted frequency and the envelope spectra are presented on the figures as half-width of the spectra. Some typical correlograms and resulting power spectra are presented in Figs. 5 to 12. A value of q = 100 was used for all calculations. The results corresponding to readings every 0.1 second which give f_m = 5 cps are

shown by the heavy lines. The results corresponding to readings every 0.5 second which yield f_m = 1 cps are shown by the dotted lines. For Figs. 5 and 6 the autocorrelation coefficient never reached zero. For Figs. 7 and 8 the autocorrelation coefficient for the 0.5 second interval data crosses zero three times. Figs. 9 and 10 were chosen to show the results for a weak signal that is just comfortably out of the noise. The autocorrelation oscillates but does not cross zero. The autocorrelation of Fig. 11 has ten crossings of the zero for the 0.5-second interval data and even two

crossings for the 0.1-second interval data. Consequently both spectra (see Fig. 12) show a peak for this 700 cps sound near 0.1 cps. Figure 13 shows another spectrum for 1200 cps sound which also exhibits a significant peak near 0.1 cps. In general the spectra did not indicate significant peaks and appeared similar to Figure 14 which is a typical example.

All of the spectra were plotted on logarithmic paper. These spectra plots generally could be roughly fitted with a straight line for difference frequencies greater than 0.1 cps. Most of the curves fell off with the inverse cube of the difference frequency similar to Figures 6 and 13. Some curves could be better ~~xx/xxx~~ represented by an inverse square dependence such as Figures 8 and 10 and a few by an inverse fourth power dependence. It was found that the spreading varied almost linearly with the frequency transmitted. For relative powers, P, less than 5×10^{-1} the relationship for these long tones half-spectra width can be approximated by

$$P = b f_o \left| f - f_o \right|^{-3} \tag{15}$$

where f_o is the transmitted frequency in cps and f is the frequency of interest in cps.

All of the data were fitted with Equation (15) to determine the value of b. There was no significant dependence of b on either range or hydrophone depth. The values of b exhibited considerable variability which could obscure a smaller dependence. The values of b were in general higher for the sandstone bottom than for the sand bottom. The value of b for the sandstone bottom is $b = (13.9 \pm 2.7) \times 10^{-6}$. The value for the sand bottom is $b = (7.7 \pm 0.8) \times 10^{-6}$. The overall average is $b = (10.1 \pm 1.2) \times 10^{-6}$.

Equation (15) is not a perfect representation of all the data and to describe the conditions individually the slightly smoothed power spectra data are summarized in Tables III and IV where the 10-db, 20-db, and 30-db down points are tabulated for the analysis with $\Delta f = 0.05$ cps. For some cases, the 30-db down point could not be determined because of noise. For these cases the noise level in db is tabulated in place of the spectra width at the 30-db down point.

BEAT FREQUENCY SPECTRA

Some data were obtained for the purpose of checking the symmetry of the power spectra. An analysis of the received signal envelope of course yields spectra which are symmetrical about zero. It is possible that the spectra might not be symmetrical about f_o. Some special measurements were made over both bottoms to obtain the frequency distribution in a different manner. The received signal was mixed after reception with a slightly displaced frequency f_d and recorded. The analysis of the beat-frequency envelopes gives the spectra centered on $f_d - f_o$ of the received signals. Any assymmetry will be shown by these beat-frequency spectra. The analysis was performed on the envelope of the beat-frequency signal with the equations of the preceding section.

The results for two successive 5-minute 700 cps tones are shown in Fig. 15. The solid curve gives the results of the regular analysis of the signal envelope. The dashed and dotted curves give the result of analysis of the received signal mixed with a 701.15 cps signal and are displaced 1.15 cps for plotting. The dotted curve is the mirror image of the

15

spectra below 700 cps. It stops, of course, at a frequency corresponding to zero in the regular analysis. A comparison of the dashed and dotted beat-frequency analysis curves indicates no significant assymmetry. The results of the signal envelope analysis of a preceeding signal agrees fairly well down 20 db. The departures for frequencies greater than 1 cps is due to the fact that frequency f_d was only 1.15 cps from f_o.

ACKNOWLEDGMENTS

The author wishes to thank Mr. R. J. Bolam, A. Davis, G. S. Yee, and M. D. Ward of NEL who were in charge of the receiving equipment, Mr. P. G. Hansen who obtained the data on which Figure 2 is based, Mr. E. Freedman of the Naval Ordnance Laboratory at Corona, California. The data analysis was performed by C. B. Porter and S. W. Porter of NEL.

REFERENCES

1. P. G. Hoel, Introduction to Mathematical Statistics (John Wiley & Sons, Inc., London, 1947).
2. R. B. Blackman and J. W. Tukey Bell System Tch. J. 37, 185-280 (1958).
3. R. B. Blackman and J. W. Tukey Bell System Tech. J. 37, 485-569 (1958).

ILLUSTRATIONS

ILLUSTRATIONS (Continued)

TABLE I - AMPLITUDE DISTRIBUTION CURVE PARAMETERS FOR 60-FATHOM FLAT SAND BOTTOM

Frequency (cps)	Range (kyd)	HYDROPHONE 10 FEET DEEP			HYDROPHONE 100 FEET DEEP			HYDROPHONE 200 FEET DEEP			HYDROPHONE 15 FEET FROM BOTTOM		
		V (%)	A_3	A_4-3	V (%)	A_3	A_4-3	V (%)	A_3	A_4-3	V (%)	A_3	A_4-3
350	10	--	--	--	29.9	0.10	-0.25	46.7	0.01	-0.63	35.8	-0.21	0.57
350	15	49.5	0.33	-0.18	33.3	-0.04	-0.35	52.2	0.12	-0.60	33.6	0.22	0.30
350	20	56.7	0.51	-0.17	33.8	-0.04	0.02	33.3	-0.51	0.06	46.9	0.17	-0.46
350	30	47.1	0.33	-0.22	27.1	-0.44	0.99	41.0	0.16	-0.31	43.3	0.31	-0.14
700	10	--	--	--	34.6	-0.14	-0.45	63.2	0.55	-0.38	49.5	0.47	-0.06
700	15	51.5	0.23	-0.49	49.5	0.36	0.19	53.2	0.27	-0.42	51.9	0.50	-0.25
700	20	46.9	-0.02	-0.64	34.6	0.05	0.28	30.1	-0.24	0.33	45.8	0.13	-0.75
700	30	37.2	0.03	-0.39	54.7	0.40	-0.10	43.4	0.15	-0.39	46.8	0.11	-0.77
1200	10	34.8	-0.24	-0.17	40.9	0.04	-0.48	43.8	-0.29	-0.78	42.3	0.25	-0.30
1200	15	40.2	0.05	-0.06	38.7	0.03	0.33	56.4	0.42	0.02	47.7	0.37	-0.05
1200	20	53.7	0.28	-0.49	47.6	0.27	-0.13	64.5	0.69	0.82	41.0	0.29	-0.04
1200	30	49.5	0.44	-0.10	42.4	0.10	-0.44	47.8	0.42	0.11	50.1	0.32	-0.49
2400	10	36.2	0.07	-0.41	29.1	0.00	-0.49	58.2	0.55	0.05	45.2	0.26	-0.32
2400	15	31.1	-0.20	0.14	37.2	0.05	-0.16	--	--	--	48.4	0.33	-0.53
2400	30	45.8	0.35	-0.25	35.0	0.14	0.04	52.5	0.70	0.69	47.5	0.35	-0.30

TABLE II - AMPLITUDE DISTRIBUTION CURVE PARAMETERS FOR 50-FATHOM MIOCENE SANDSTONE BOTTOM

Frequency (cps)	Range (kyd)	HYDROPHONE 10 FEET DEEP			HYDROPHONE 100 FEET DEEP			HYDROPHONE 200 FEET DEEP			HYDROPHONE 15 feet FROM BOTTOM		
		V (%)	A_3	A_4-3	V (%)	A_3	A_4-3	V (%)	A_3	A_4-3	V (%)	A_3	A_4-3
350	4	47.2	0.85	-0.75	44.6	0.17	-0.62	42.7	-0.10	-0.93	38.4	-0.19	-0.64
350	8	48.6	0.36	-0.69	40.5	-0.02	-0.58	—	—	—	44.2	0.06	-0.78
350	16	45.1	0.48	0.33	—	—	—	—	—	—	22.7	-0.25	-0.18
350	25	28.0	-0.46	[illegible]	24.9	-0.39	-0.24	9.6	-0.78	0.33	50.1	0.33	-0.22
700	4	33.3	-0.30	0.60	28.8	-0.36	0.37	12.4	-0.69	-0.38	48.5	0.38	-0.03
700	8	—	—	—	39.6	-0.18	-0.42	—	—	—	36.3	-0.31	-0.51
700	16	60.4	0.53	-0.34	37.3	-0.09	-0.35	—	—	—	44.9	0.16	-0.77
700	25	50.9	0.11	-0.53	40.6	-0.66	-0.58	—	—	—	—	—	—
1400	4	45.5	0.18	-0.34	42.6	0.03	-0.65	51.2	-0.08	-1.08	43.0	0.01	-0.61
1400	16	56.3	0.46	-0.38	45.3	0.02	-0.90	57.2	0.44	-0.65	36.8	0.48	-0.35
2800	4	58.3	0.40	-0.49	51.7	0.46	0.21	50.3	0.13	-0.72	46.5	0.26	-0.51

TABLE XXI - SPECTRA HALF-WIDTHS IN C/S FOR 60-FATHOM FLAT SAND BOTTOM

Frequency (c/s)	Range (kyds)	Hydrophone 10 Feet Deep -10db	Hydrophone 10 Feet Deep -20db	Hydrophone 10 Feet Deep -30db	Hydrophone 100 Feet Deep -10db	Hydrophone 100 Feet Deep -20db	Hydrophone 100 Feet Deep -30db	Hydrophone 200 Feet Deep -10db	Hydrophone 200 Feet Deep -20db	Hydrophone 200 Feet Deep -30db	Hydrophone 15 Feet From Bottom -10db	Hydrophone 15 Feet From Bottom -20db	Hydrophone 15 Feet From Bottom -30db
350	10	—	—	—	0.30	0.55	0.80	0.35	0.70	1.05	0.35	0.70	2.05
350	15	0.35	0.65	1.15	0.30	0.55	0.95	0.30	0.65	1.15	0.40	0.65	1.40
350	20	0.30	0.60	-20db*	0.30	0.65	-23db*	0.30	0.60	[illegible]	0.45	0.85	[illegible]
350	30	0.40	0.70	-20db*	0.30	0.65	-24db*	0.35	0.65	-24db*	0.40	0.75	-22db*
700	10	—	—	—	0.40	0.95	1.40	0.55	1.10	1.65	0.65	1.15	1.90
700	15	0.45	0.95	-26db*	0.40	0.90	-28db*	0.50	1.05	-27db*	0.55	1.05	-29db*
700	20	0.30	0.80	-25db*	0.50	1.00	-22db*	0.40	0.90	-23db*	0.15	0.65	1.50**
700	30	0.40	0.85	1.25	0.50	1.00	1.65	0.40	0.90	1.40	0.35	0.75	1.40
1200	10	0.50	1.10	1.80	0.50	1.10	1.75	0.45	1.00	1.75	0.45	1.05	1.65
1200	15	0.30	0.85	-25db*	0.20	0.90	-25db*	0.30	1.00	-25db*	0.60	1.60	-22db*
1200	20	0.15	0.60	1.45	0.50	1.20	2.30**	0.60	1.85	-22db*	0.55	1.35	-23db*
1200	30	0.65	1.50	2.50**	0.55	1.15	1.90**	0.60	1.20	2.10	0.35	1.05	1.90
2400	10	0.25	0.85	1.95	0.25	0.75	1.75	[illegible]	1.50	2.80	0.35	1.25	2.85
2400	15	0.50	1.35	2.65	0.30	1.00	2.00	—	—	—	0.55	1.35	2.75
2400	30	0.55	1.25	2.50	0.55	1.40	2.50	0.60	1.50	2.70	0.35	1.15	2.30

*Noise level
**At Noise

TABLE IV - SPECTRA HALF-WIDTHS IN C/S FOR 50-FATHOM MIOCENE SANDSTONE BOTTOM

Frequency (c/s)	Range (kyds)	HYDROPHONE 10 FEET DEEP			HYDROPHONE 100 FEET DEEP			HYDROPHONE 200 FEET DEEP			HYDROPHONE 15 FEET FROM BOTTOM		
		-10 db	-20 db	-30 db	-10 db	-20 db	-30 db	-10 db	-20 db	-30 db	-10 db	-20 db	-30 db
350	4	0.45	1.25	-22 db*	0.30	0.70	-29 db*	0.40	0.95	-23 db*	0.35	0.75	-29 db*
350	8	0.15	0.55	-29 db*	0.25	0.65	1.50 **	--	--	--	0.15	0.50	1.00
350	16	0.35	0.95	-23 db*	--	--	--	--	--	--	0.15	0.55	-28 db*
350	25	0.10	0.45	1.05	0.30	0.60	1.15	0.20	0.55	1.20	0.20	0.60	1.05
700	4	0.10	0.35	0.85	0.25	0.55	1.10	0.10	0.45	0.90	0.20	0.60	1.05
700	8	--	--	--	0.25	0.60	1.10	--	--	--	0.15	0.45	0.85
700	16	0.35	0.95	1.75	0.20	0.55	1.00	--	--	--	0.25	0.65	1.15
700	25	0.40	1.20	-26 db*	0.10	0.30	0.90	--	--	--	--	--	--
1200	4	0.50	1.40	2.25	0.45	1.35	2.40	0.10	0.85	1.80	0.35	1.30	2.30
1200	16	0.37	1.35	2.00	0.20	0.90	1.70	0.15	0.80	1.60	0.10	0.40	1.25
2400	4	0.45	2.00	4.50	0.65	2.70	5	0.60	2.50	5	0.70	2.60	5

* Noise Level
** At Noise

TABLE V - CROSS CORRELATIONS OF VARIOUS HYDROPHONES FOR 60-FATHOM FLAT SAND BOTTOM

Frequency (cps)	Range (kyds)	DEPTHS OF HYDROPHONES 10 & 100 FEET	10 & 200 FEET	10 & 345 FEET	100 & 200 FEET	100 & 345 FEET	200 & 345 FEET
350	10	--	--	--	0.185	0.067	0.232
350	15	-0.183	-0.004	0.060	-0.034	0.146	0.090
350	20	-0.123	0.094	0.076	0.291	-0.187	-0.068
350	30	-0.140	0.248	0.056	-0.222	-0.034	-0.125
700	10	--	--	--	-0.034	-0.090	-0.012
700	15	-0.150	0.004	-0.084	0.036	0.118	0.186
700	20	-0.049	0.134	0.226	0.029	0.077	0.121
700	30	-0.041	0.034	-0.025	0.034	-0.073	-0.043
1200	10	0.040	-0.059	0.086	-0.017	0.123	0.105
1200	15	0.294	0.306	-0.042	0.166	-0.130	-0.102
1200	20	-0.204	-0.151	0.037	-0.022	0.000	-0.040
1200	30	0.066	0.023	-0.031	-0.034	-0.016	0.064
2400	10	-0.455	0.125	0.246	-0.153	-0.365	0.148
2400	15	0.106	-0.059	0.151	0.096	0.149	0.071
2400	20	-0.085	-0.098	-0.120	0.135	0.087	0.173
2400	30	-0.181	-0.001	-0.053	0.030	0.026	0.156

TABLE VII - CROSS CORRELATIONS OF VARIOUS HYDROPHONES FOR 50-FATHOM MIOCENE SANDSTONE BOTTOM

Frequency (cps)	Range (kyds)	Depths of Hydrophones: 10 & 100 FEET	10 & 200 FEET	10 & 345 FEET	100 & 200 FEET	100 & 345 FEET	200 & 345 FEET
350	4	-0.069	0.024	0.013	0.043	-0.116	-0.022
350	8	-0.189	--	-0.004	--	0.168	--
350	16	--	--	-0.050	--	--	--
350	25	-0.150	0.254	-0.154	0.194	0.066	0.007
700	4	0.115	0.480	-0.084	0.420	0.061	0.053
700	8	--	--	--	--	0.249	--
700	16	0.421	--	0.228	--	0.401	--
700	25	-0.199	--	--	--	--	--
1200	4	-0.043	0.169	0.091	-0.165	-0.084	0.016
1200	16	-0.004	-0.178	-0.059	-0.171	-0.192	0.429
2400	4	0.156	0.185	-0.106	0.088	-0.053	-0.134
2400	16	0.536	0.519	0.364	0.574	0.408	0.413

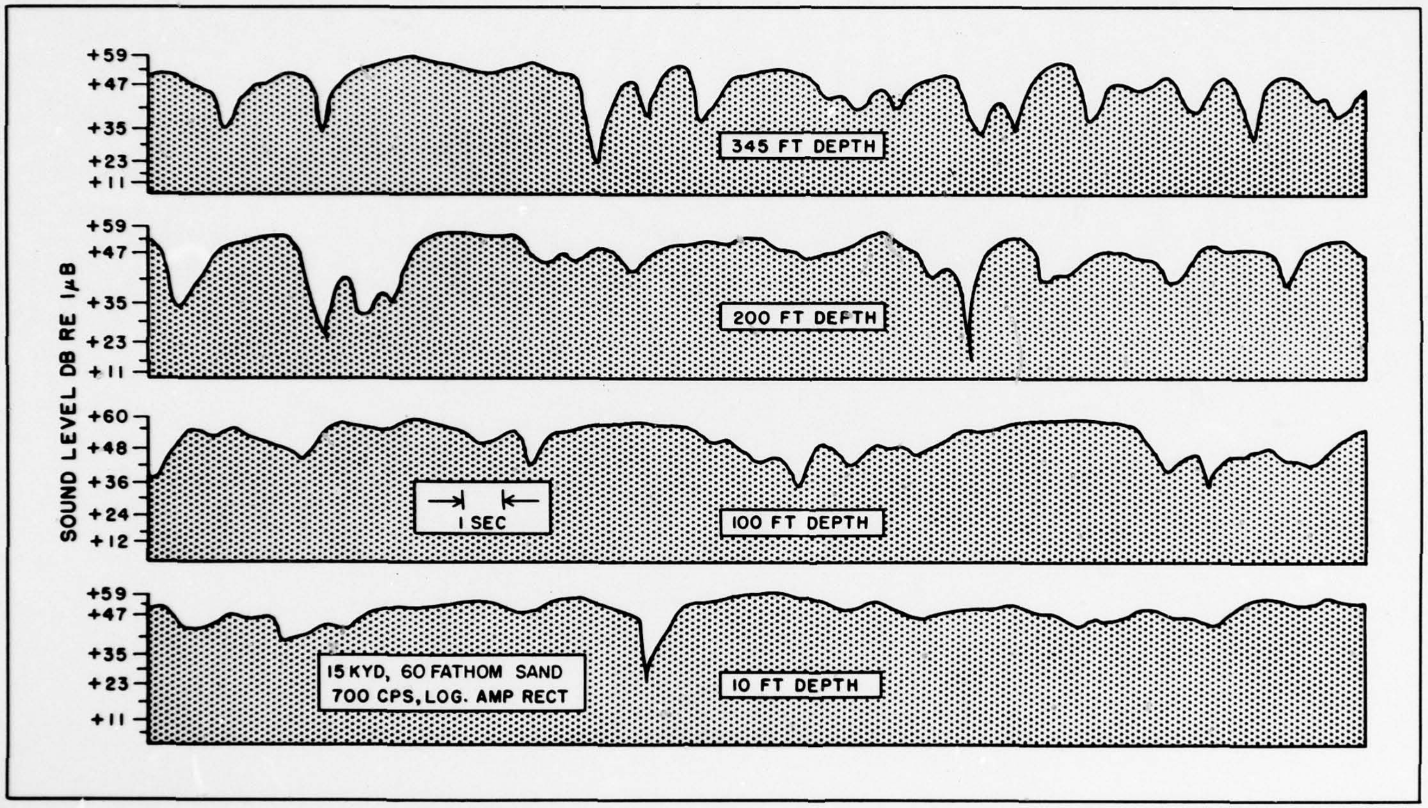
SOUND LEVEL DB RE 1 μB
+59
+47
+35
+23
+11
345 FT DEPTH
+59
+47
+35
+23
+11
200 FT DEPTH
+60
+48
+36
+24
+12
1 SEC
100 FT DEPTH
+59
+47
+35
+23
+11
15 KYD, 60 FATHOM SAND
700 CPS, LOG. AMP RECT
10 FT DEPTH

FIG. 1

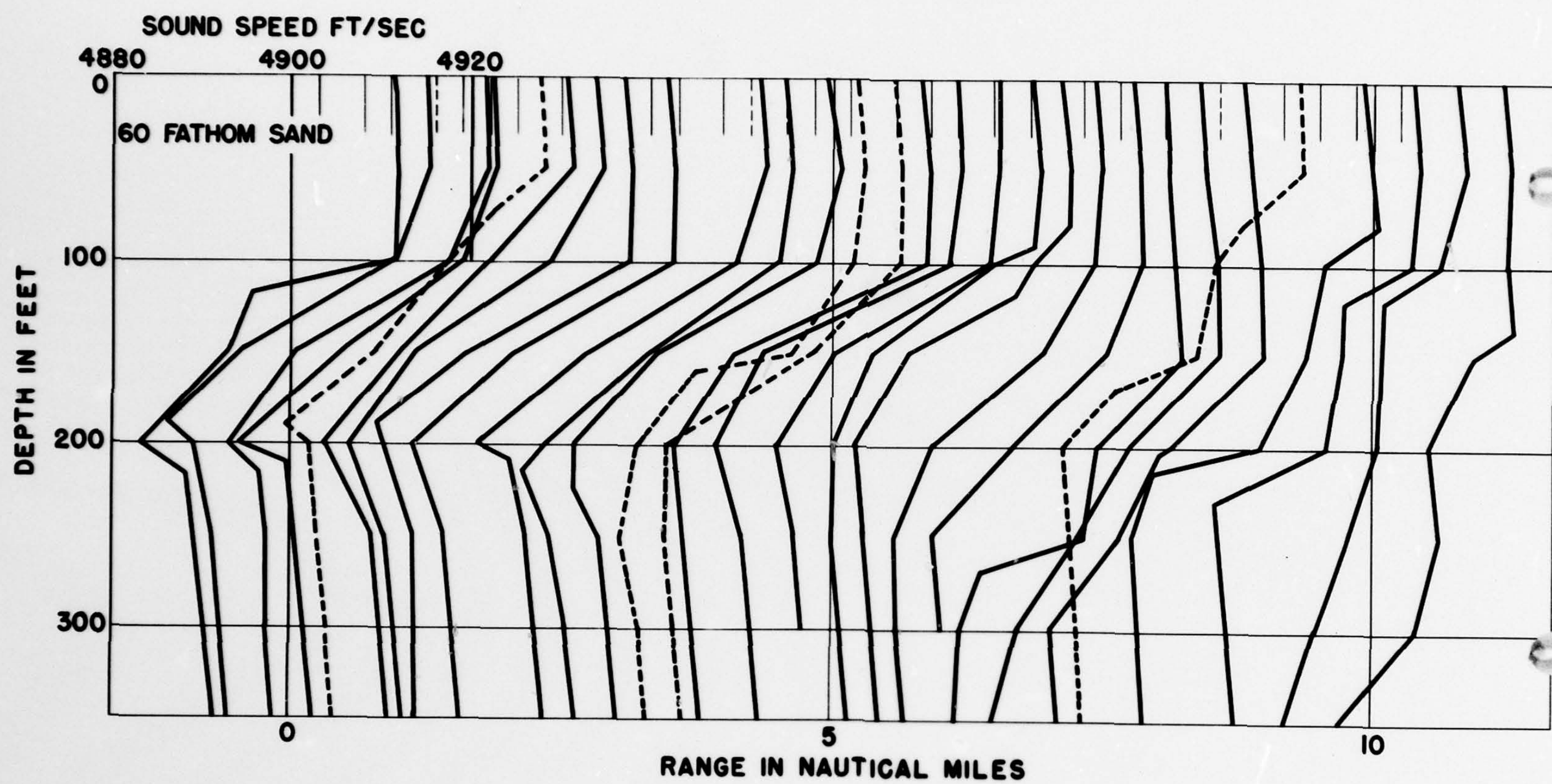
SOUND SPEED FT/SEC
4880
4900
4920
0
100
200
300
DEPTH IN FEET
60 FATHOM SAND
0
5
10
RANGE IN NAUTICAL MILES

FIG. 2

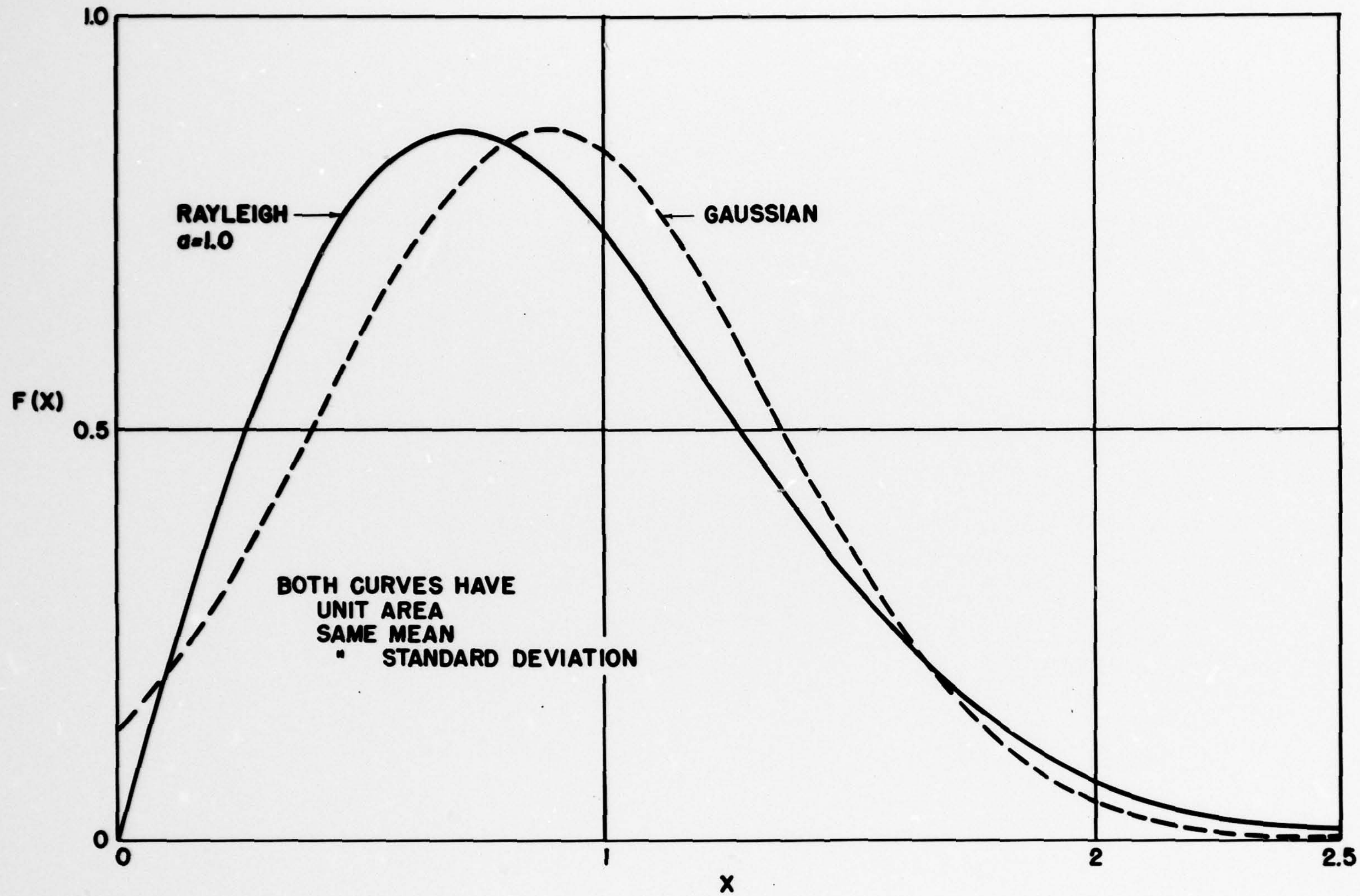
1.0
F (X)
0.5
0
0
1
2
2.5
X
RAYLEIGH
a=1.0
GAUSSIAN
BOTH CURVES HAVE
UNIT AREA
SAME MEAN
" STANDARD DEVIATION

FIG. 3

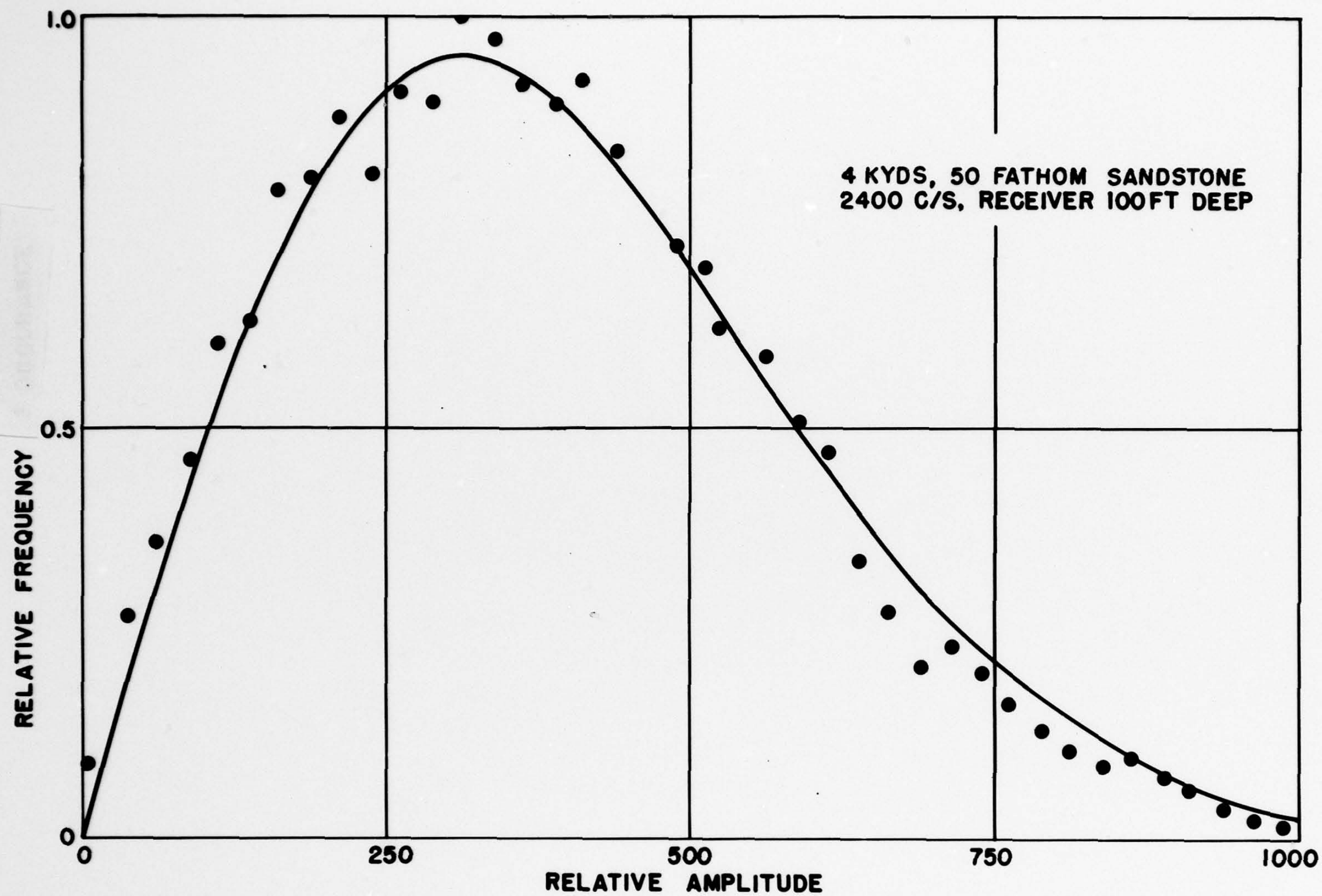
4 KYDS, 50 FATHOM SANDSTONE
2400 C/S, RECEIVER 100FT DEEP
1.0
0.5
0
RELATIVE FREQUENCY
0
250
500
750
1000
RELATIVE AMPLITUDE

FIG. ~~3~~ 4

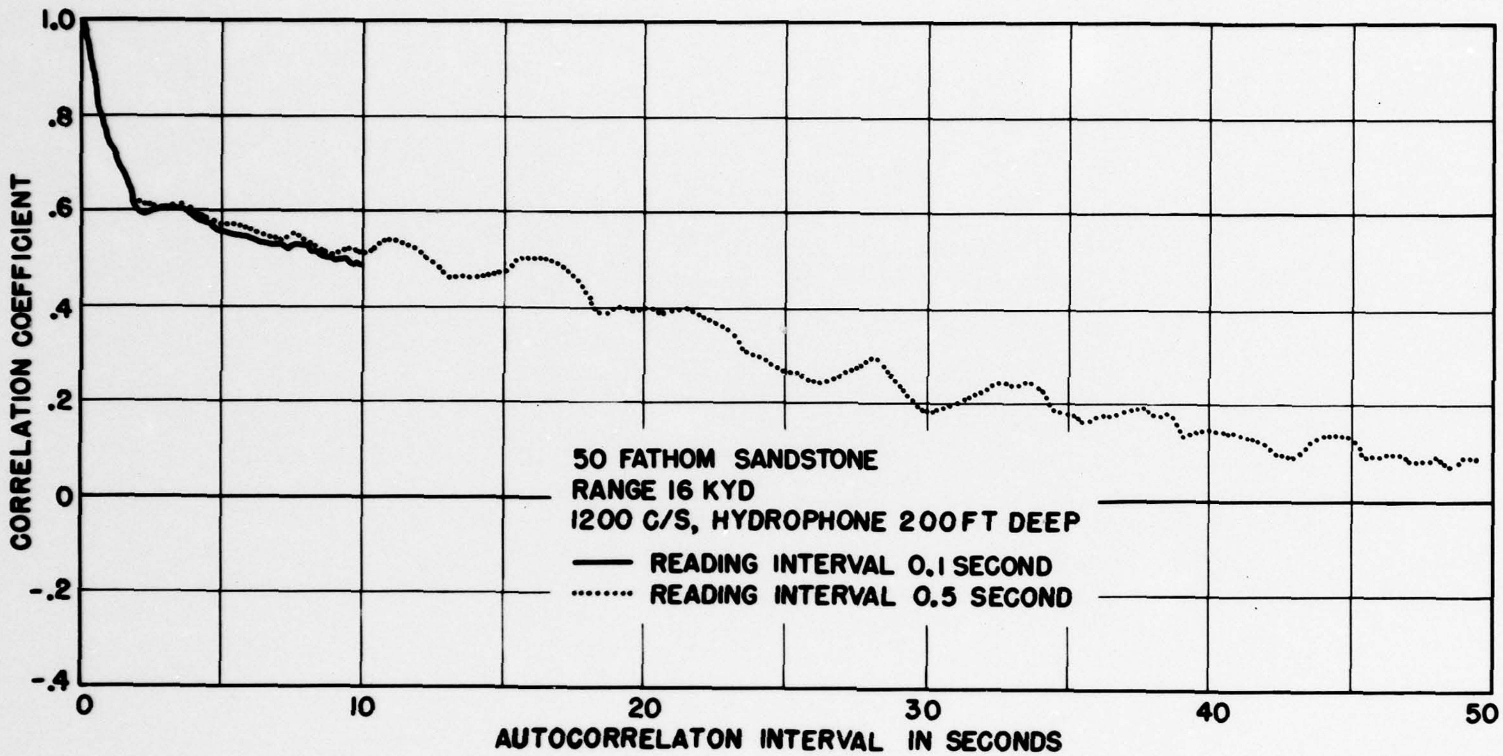

1.0
.8
.6
.4
.2
0
-.2
-.4
CORRELATION COEFFICIENT
0
10
20
30
40
50
AUTOCORRELATON INTERVAL IN SECONDS
50 FATHOM SANDSTONE
RANGE 16 KYD
1200 C/S, HYDROPHONE 200FT DEEP
READING INTERVAL 0.1 SECOND
READING INTERVAL 0.5 SECOND

FIG. 5

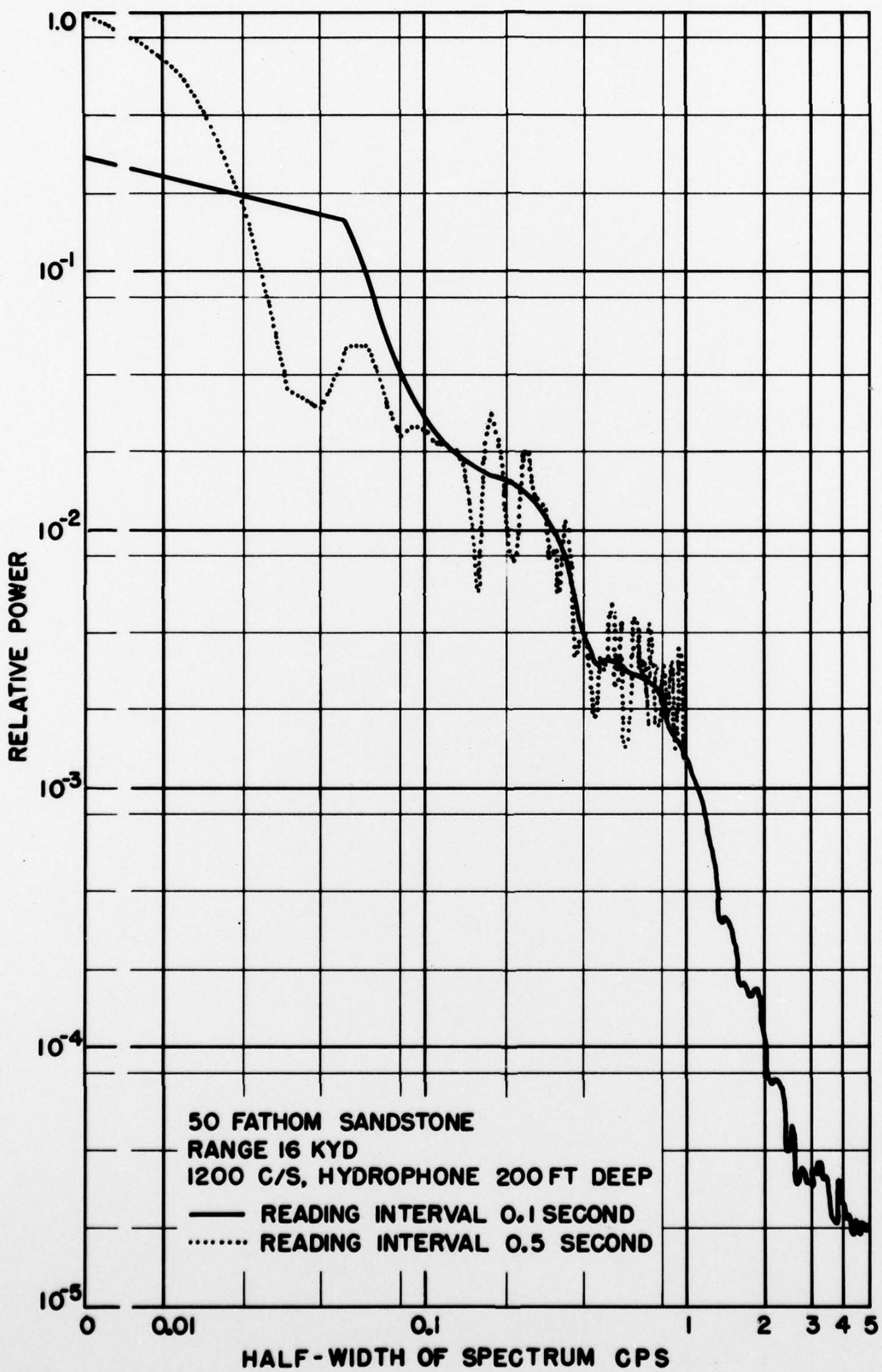

1.0
10^{-1}
10^{-2}
10^{-3}
10^{-4}
10^{-5}
RELATIVE POWER
0
0.01
0.1
1
2
3
4
5
HALF-WIDTH OF SPECTRUM CPS
50 FATHOM SANDSTONE
RANGE 16 KYD
1200 C/S, HYDROPHONE 200 FT DEEP
READING INTERVAL 0.1 SECOND
READING INTERVAL 0.5 SECOND

FIG. ~~5~~ 6

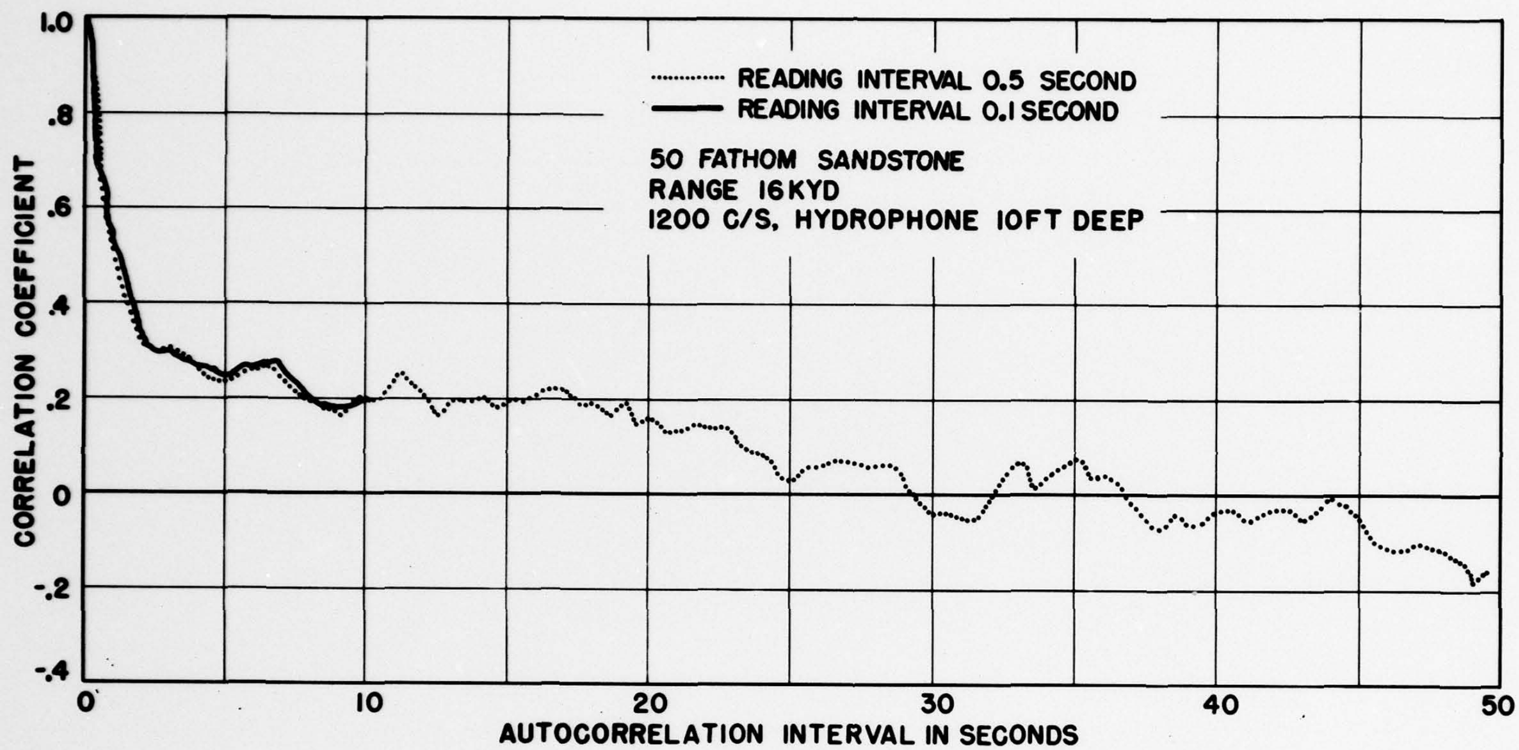
READING INTERVAL 0.5 SECOND
READING INTERVAL 0.1 SECOND
50 FATHOM SANDSTONE
RANGE 16 KYD
1200 C/S, HYDROPHONE 10 FT DEEP
CORRELATION COEFFICIENT
1.0
.8
.6
.4
.2
0
-.2
-.4
0
10
20
30
40
50
AUTOCORRELATION INTERVAL IN SECONDS

FIG. ~~6~~ 7

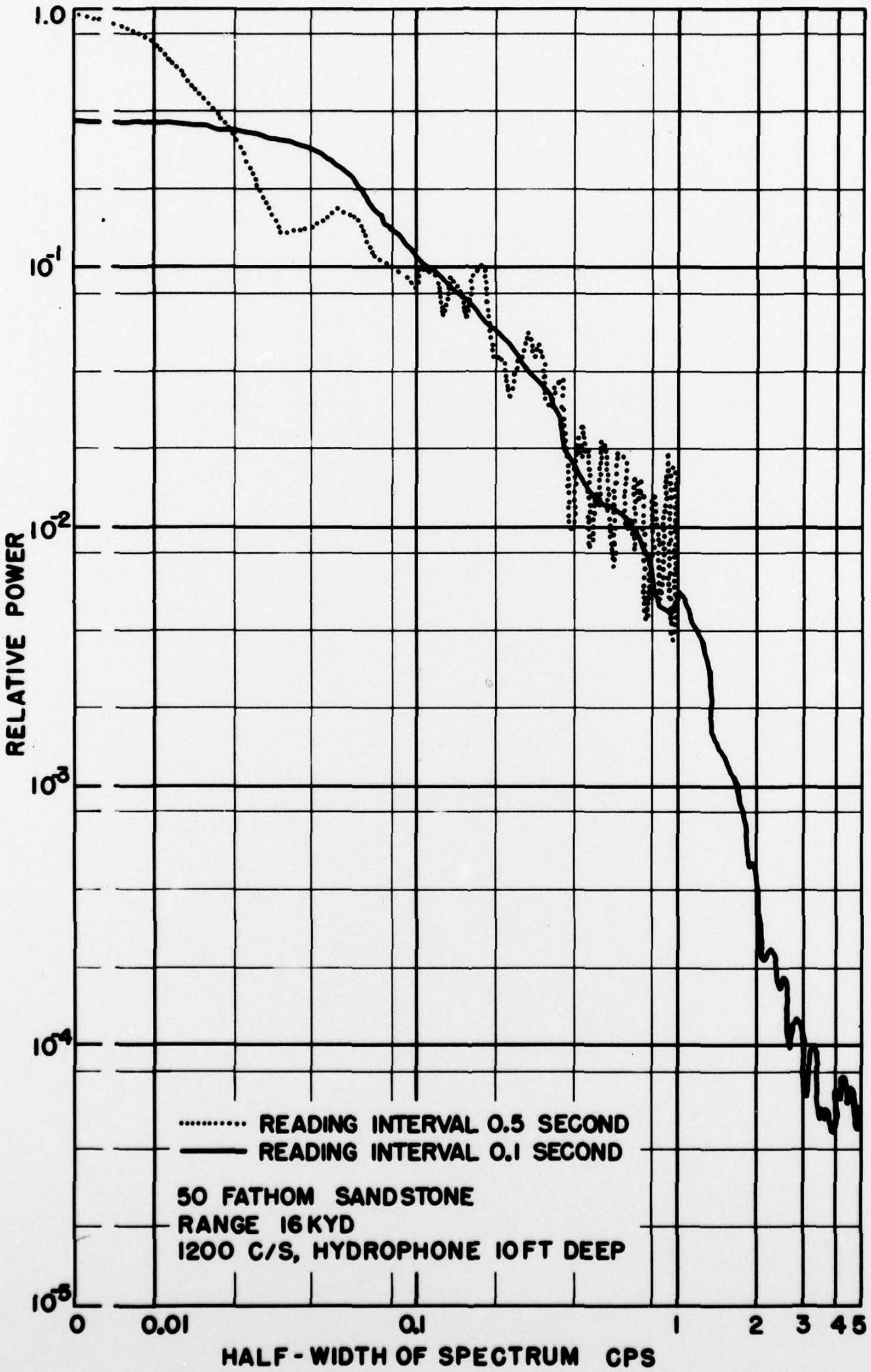

1.0
10⁻¹
10⁻²
10⁻³
10⁻⁴
10⁻⁵
RELATIVE POWER
READING INTERVAL 0.5 SECOND
READING INTERVAL 0.1 SECOND
50 FATHOM SANDSTONE
RANGE 16 KYD
1200 C/S, HYDROPHONE 10 FT DEEP
0
0.01
0.1
1
2
3
4
5
HALF - WIDTH OF SPECTRUM CPS

FIG. ~~7~~ 8

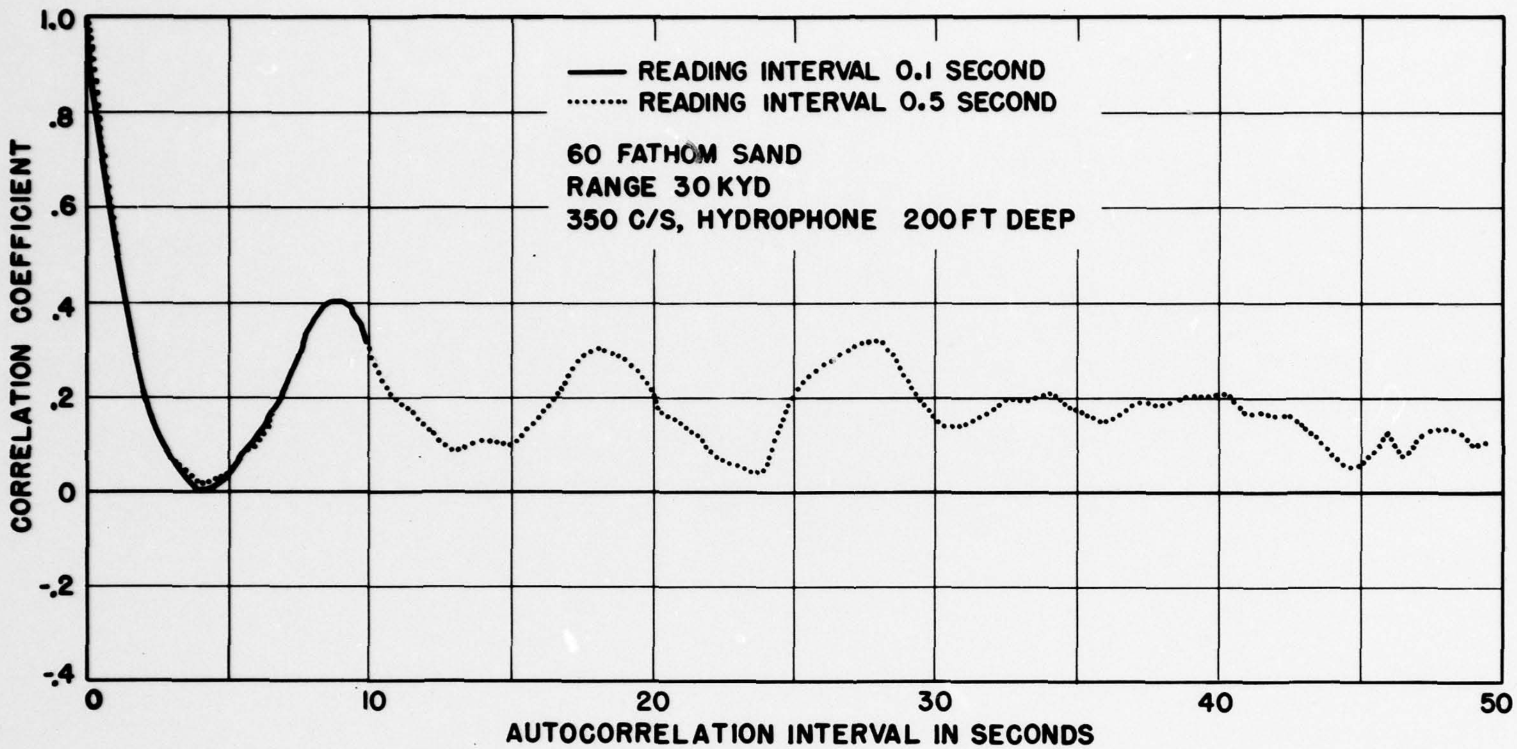
READING INTERVAL 0.1 SECOND
READING INTERVAL 0.5 SECOND
60 FATHOM SAND
RANGE 30 KYD
350 C/S, HYDROPHONE 200 FT DEEP
CORRELATION COEFFICIENT
1.0
.8
.6
.4
.2
0
-.2
-.4
0
10
20
30
40
50
AUTOCORRELATION INTERVAL IN SECONDS

FIG. ~~8~~ 9

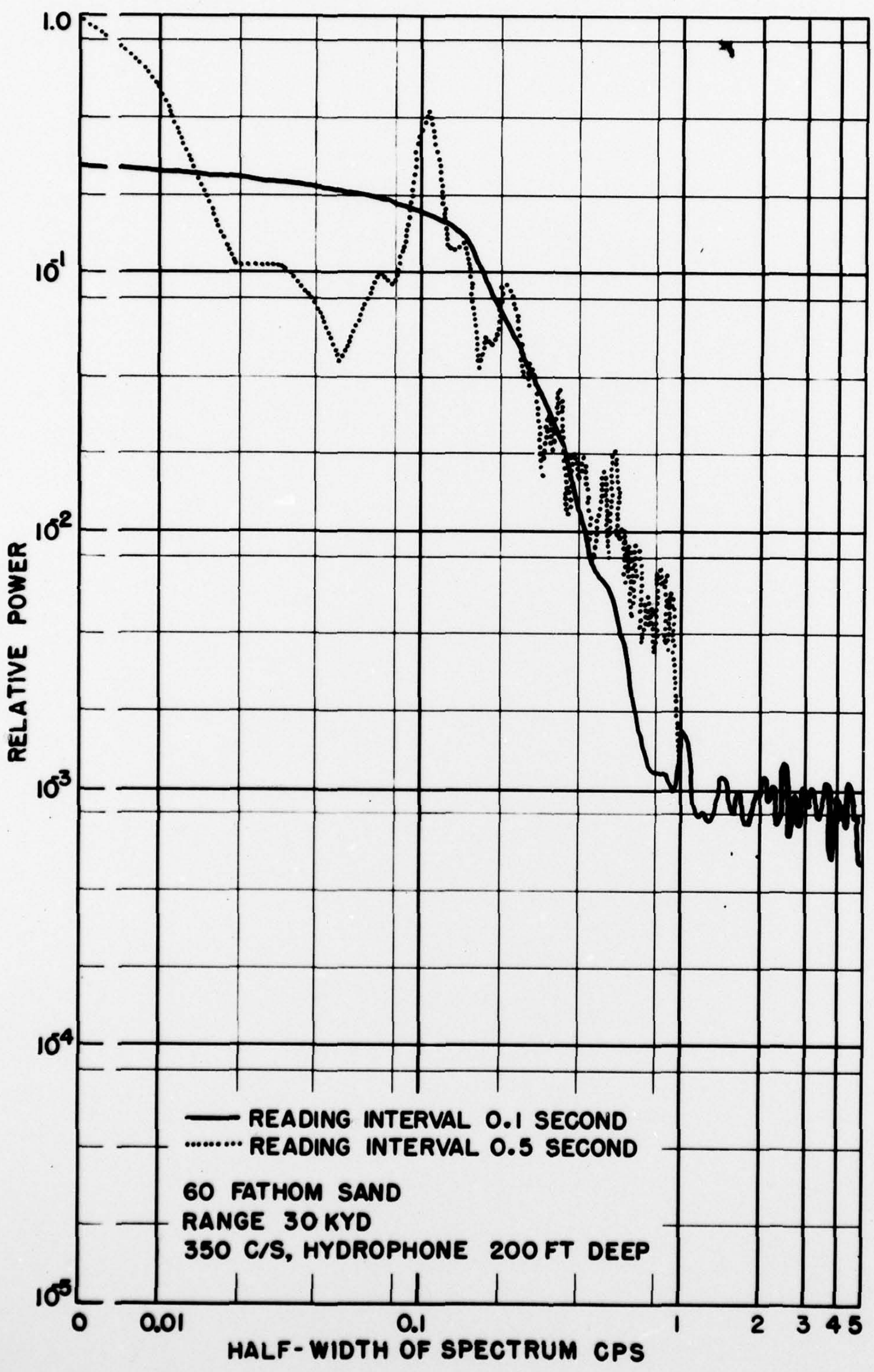

1.0
10^{-1}
10^{-2}
10^{-3}
10^{-4}
10^{-5}
RELATIVE POWER
0
0.01
0.1
1
2
3
4
5
HALF-WIDTH OF SPECTRUM CPS
READING INTERVAL 0.1 SECOND
READING INTERVAL 0.5 SECOND
60 FATHOM SAND
RANGE 30 KYD
350 C/S, HYDROPHONE 200 FT DEEP

FIG. ~~9~~ 10

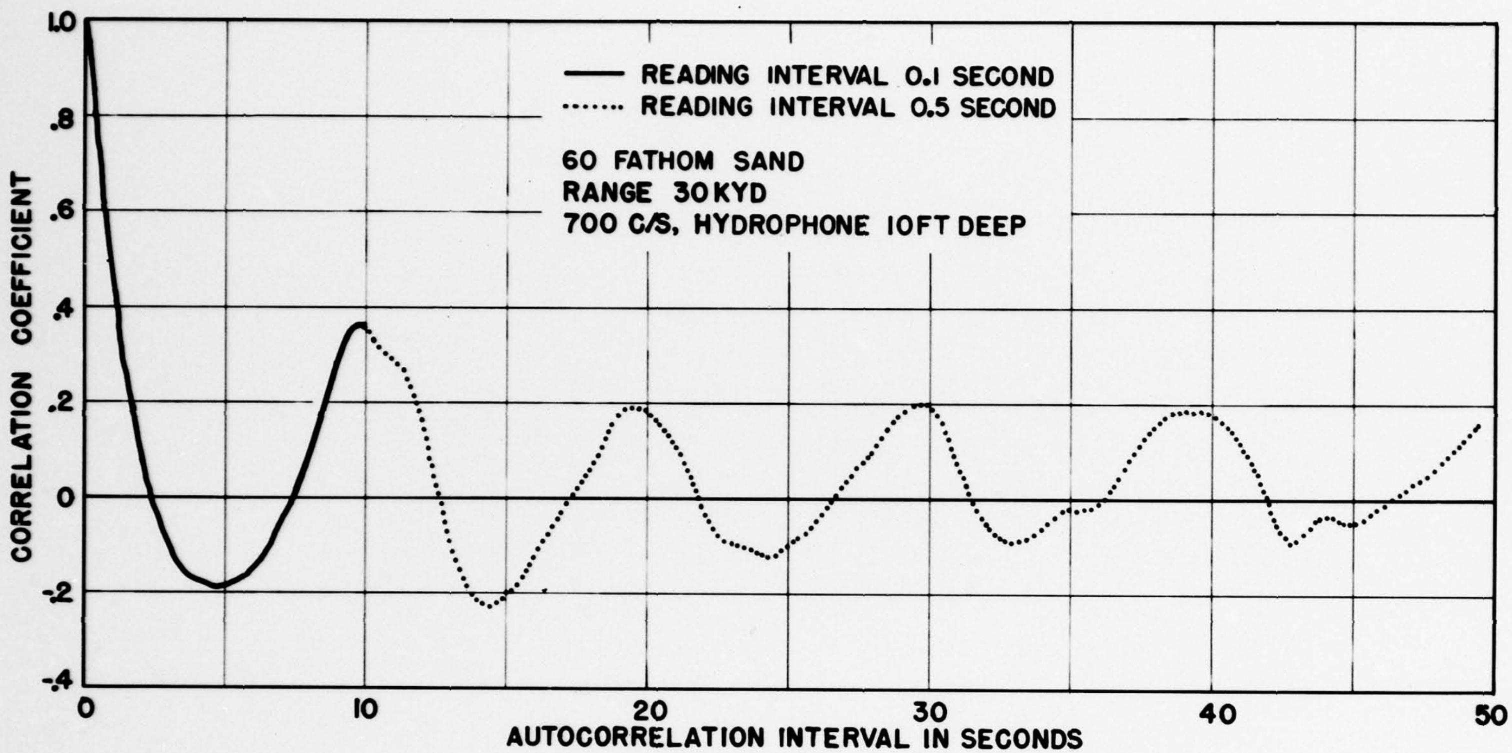

1.0
.8
.6
.4
.2
0
-.2
-.4
CORRELATION COEFFICIENT
0
10
20
30
40
50
AUTOCORRELATION INTERVAL IN SECONDS
READING INTERVAL 0.1 SECOND
READING INTERVAL 0.5 SECOND
60 FATHOM SAND
RANGE 30 KYD
700 C/S, HYDROPHONE 10 FT DEEP

FIG. ~~10~~ 11

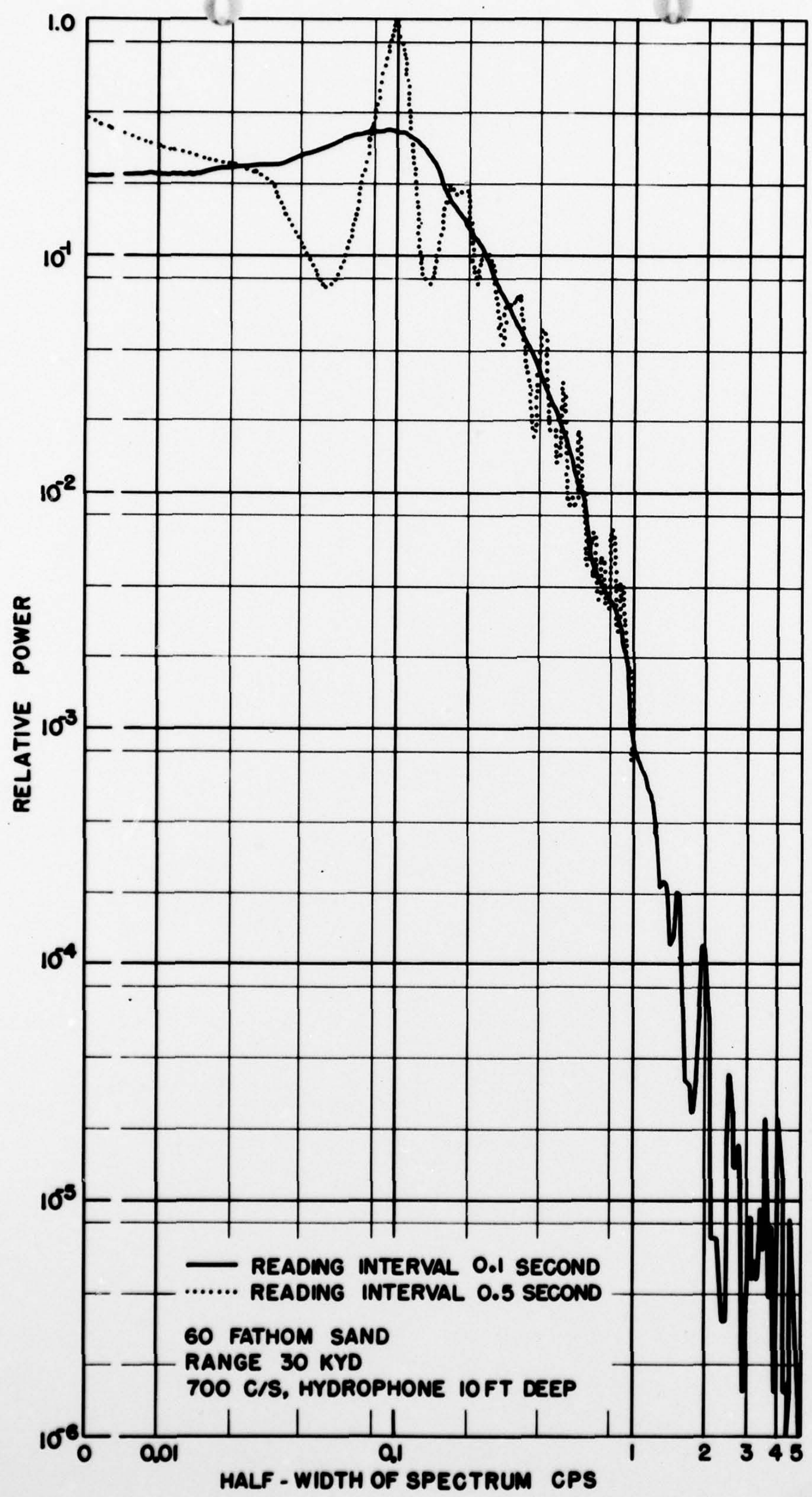

1.0
10^{-1}
10^{-2}
10^{-3}
10^{-4}
10^{-5}
10^{-6}
RELATIVE POWER
READING INTERVAL 0.1 SECOND
READING INTERVAL 0.5 SECOND
60 FATHOM SAND
RANGE 30 KYD
700 C/S, HYDROPHONE 10 FT DEEP
0
0.01
0.1
1
2
3
4
5
HALF - WIDTH OF SPECTRUM CPS

FIG. 12

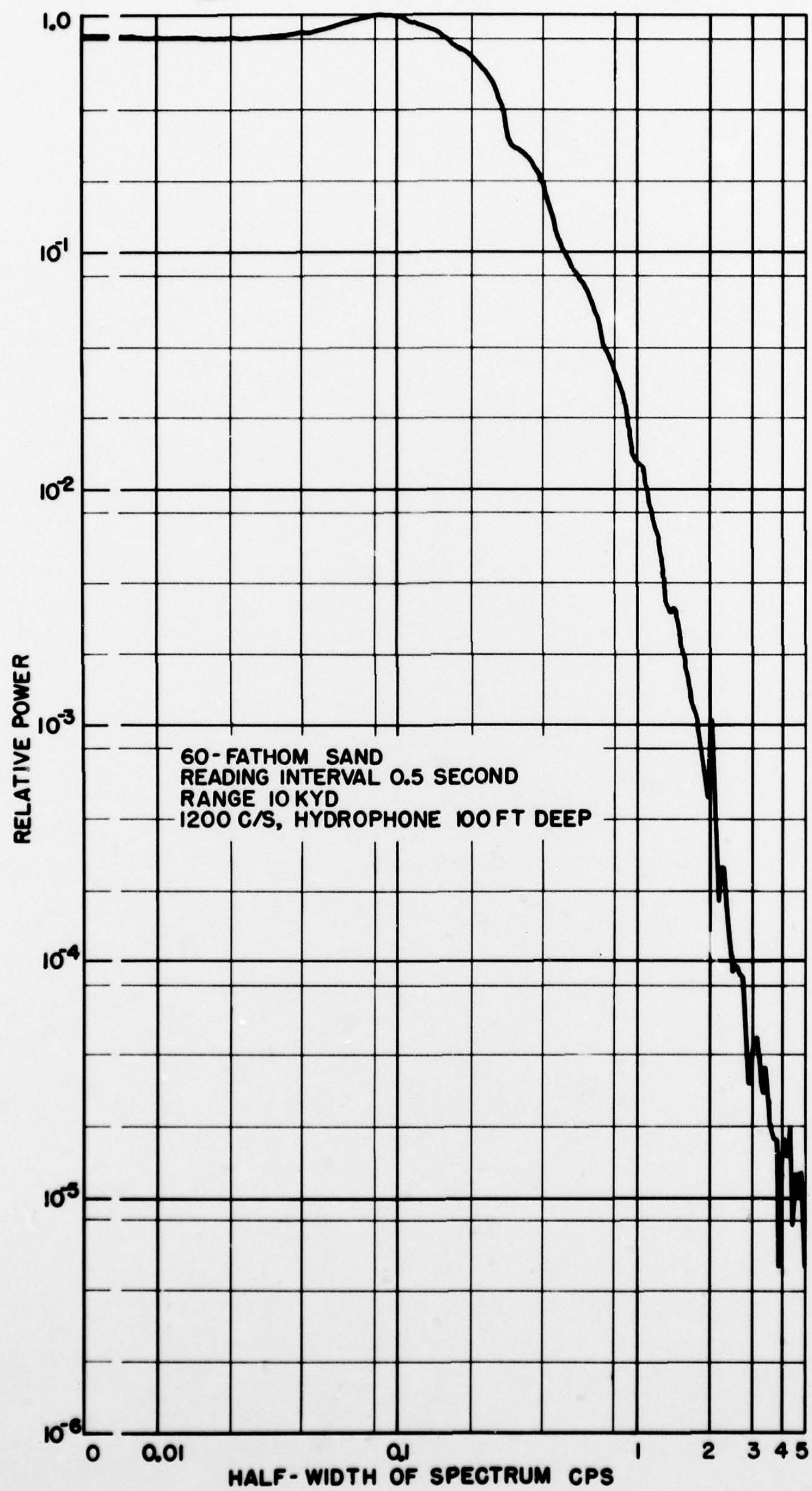
1.0
10^{-1}
10^{-2}
10^{-3}
10^{-4}
10^{-5}
10^{-6}
RELATIVE POWER
60-FATHOM SAND
READING INTERVAL 0.5 SECOND
RANGE 10 KYD
1200 C/S, HYDROPHONE 100 FT DEEP
0
0.01
0.1
1
2
3
4
5
HALF-WIDTH OF SPECTRUM CPS

FIG. ~~12~~ 13

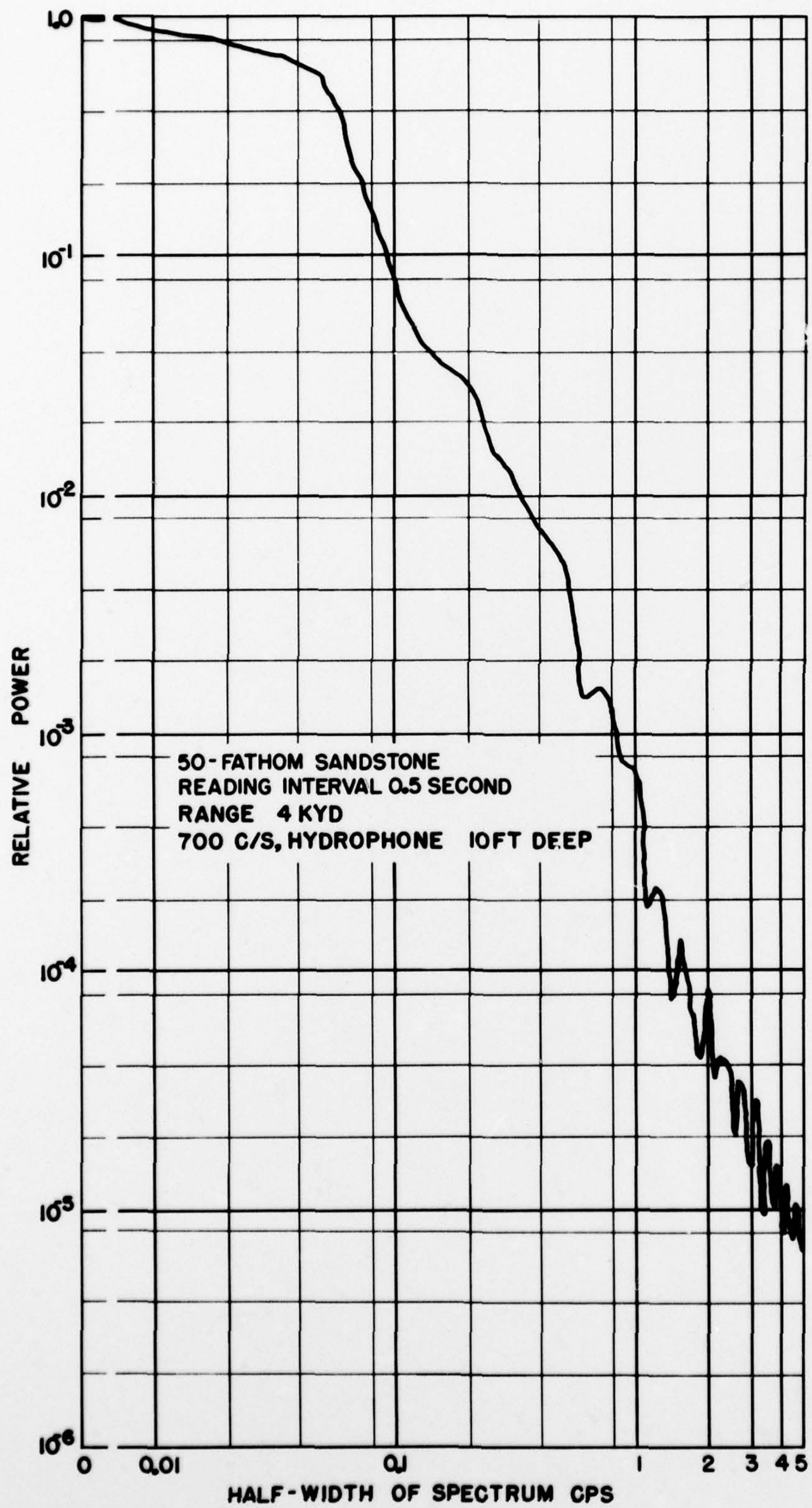

1.0
10^{-1}
10^{-2}
10^{-3}
10^{-4}
10^{-5}
10^{-6}
RELATIVE POWER
50-FATHOM SANDSTONE
READING INTERVAL 0.5 SECOND
RANGE 4 KYD
700 C/S, HYDROPHONE 10FT DEEP
0
0.01
0.1
1
2
3
4
5
HALF-WIDTH OF SPECTRUM CPS

FIG. ~~13~~ 14

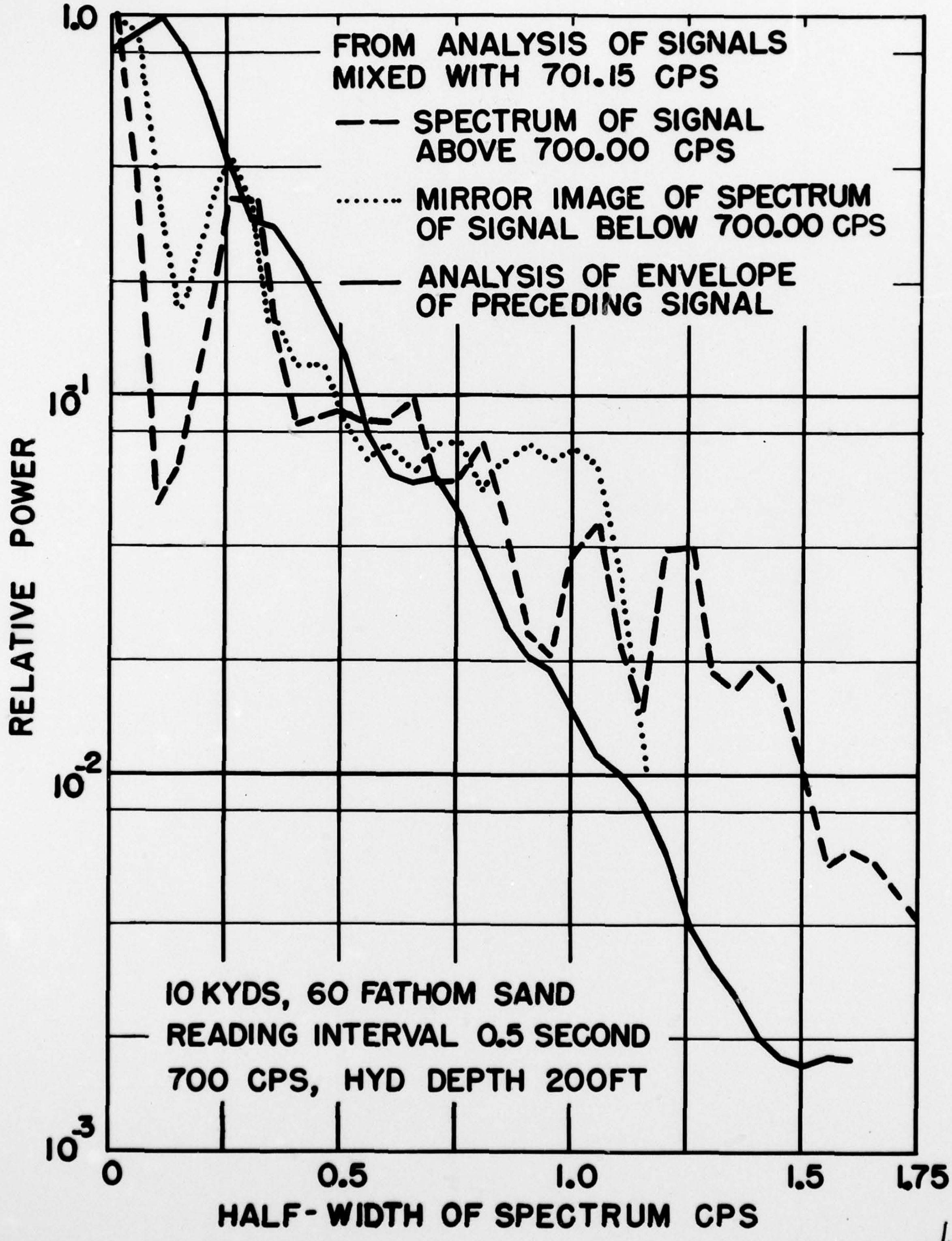

FROM ANALYSIS OF SIGNALS MIXED WITH 701.15 CPS
SPECTRUM OF SIGNAL ABOVE 700.00 CPS
MIRROR IMAGE OF SPECTRUM OF SIGNAL BELOW 700.00 CPS
ANALYSIS OF ENVELOPE OF PRECEDING SIGNAL
10 KYDS, 60 FATHOM SAND
READING INTERVAL 0.5 SECOND
700 CPS, HYD DEPTH 200FT
RELATIVE POWER
1.0
10^{-1}
10^{-2}
10^{-3}
0
0.5
1.0
1.5
1.75
HALF-WIDTH OF SPECTRUM CPS

FIG. ~~14~~ 15